

# Structure of the Galaxies in the NGC 80 Group: Two-Tiered Disks

M.A. Startseva(Ilyina)<sup>1</sup>, O.K. Sil'chenko<sup>1</sup> and A.V. Moiseev<sup>2</sup>

<sup>1</sup>*Sternberg Astronomical Institute of the Moscow State University, Moscow, Russia*

<sup>2</sup>*Special Astrophysical Observatory of the Russian Academy of Sciences, Nizhnji Arkhyz, Russia*

**Abstract.** *BV* photometric data obtained at the 6-m telescope of the Special Astrophysical Observatory are used to analyze the structure of 13 large disk galaxies in the NGC 80 group. Nine of the 13 galaxies under consideration are classified by us as lenticular galaxies. The stellar populations in the galaxies are very different, from old ones with ages of  $T > 10$  Gyrs (IC 1541) to relatively young ones with ages of  $T < 2 - 3$  Gyr (IC 1548, NGC 85). In one case, current star formation is known (UCM 0018+2216). In most of the galaxies, more precisely in all of them more luminous than  $M_B \sim -18$ , two-tiered stellar disks are detected, whose radial surface-brightness profiles can be fitted by two exponential segments with different scalelengths – shorter near the center and longer at the periphery. All dwarf S0 galaxies with single-scalelength exponential disks are close companions to giant galaxies. Except for this fact, no dependence of the properties of S0 galaxies on distance from the center of the group is found. Morphological traces of minor merger are found in the lenticular galaxy NGC 85. Basing on the last two points, we conclude that the most probable mechanisms for the transformation of spirals into lenticular galaxies in groups are gravitational ones, namely, minor mergers and tidal interactions.

# 1 INTRODUCTION

It is wide-spread opinion that lenticular galaxies, which Hubble [1] thought to be intermediate between elliptical and spiral galaxies, have appeared in the past five Gyrs which is confirmed by observations of clusters and groups at intermediate redshifts,  $z = 0.2 - 0.7$  [2, 3]. However, very different hypotheses exist about details and specific mechanisms for the transformation of spirals into lenticulars. It is clear that to transform a spiral into a lenticular galaxy, star formation must cease and the stellar disk must be dynamically heated, to eliminate spiral arms. However, it is not obvious whether it is enough only to cease star formation in the disk or whether it is necessary to increase strongly (and briefly) the intensity and efficiency of star formation at the galactic center to facilitate the growth of the bulge, which is, on average, more prominent in lenticulars than in spirals of the same mass [4, 5]. There is no observational answer to this question up to date, but we need it to identify the mechanism leading to the transformation of spirals into lenticulars. Among gasdynamical mechanisms, the ram-pressure of the hot intergalactic medium would predominantly sweep out gas of the galaxy, starving (and stopping) star formation [6], while the static pressure of the surrounding hot gas will compress the cool gas of the galactic disk, stimulating star formation [7]. As a rule, gravitational effects, such as tidal perturbation of the disk dynamics by the potential of the cluster (group) as a whole or by pair interactions between galaxies, result in formation of a central bar, with the bar then provoking the radial inflow of the outer-disk gas toward the galactic center, feeding star formation there. The outer parts of stellar disks that are devoid of gas in such way are dynamically heated, and can no longer support spiral structure [8, 9, 10]. Tidal effects also remove gas from the peripheries of galactic disks.

Just as the dominant mechanism for transformation of spirals into lenticulars is unclear, it is likewise not clear where this transformation occurs. At  $z = 0$ , lenticular galaxies are dominant in clusters, where they contribute up to 60% of all galaxy population [11, 12]. This implies that the transformation itself may occur in clusters [2, 13], especially because gasdynamical conditions (a dense, hot intergalactic medium, a high galaxy velocity dispersion) are favorable for this. However, an idea that lenticular galaxies can mainly be formed in groups has attracted more and more attention in recent years; within this paradigm, groups falling into clusters bring with them lenticular galaxies already completely formed [3]. This hypothesis is inspired by the observed morphological mix of galaxies in various types of environments at  $z = 0.3 - 0.7$ . If it is correct, it immediately distinguishes gravitational pair interactions, especially minor mergers, as the most likely mechanism for the formation of S0 galaxies, since groups display lower galaxy velocity dispersions with respect to clusters, that weaken gasdynamical effects while enhancing the effectiveness of gravitational effects. The properties of galaxies in groups are currently known not as good as the properties of galaxies in clusters which makes studies of the structure and stellar populations of lenticular galaxies in groups of key importance for further progress in understanding galaxy formation.

Table 1: Global parameters of the galaxies studied

Number <sup>1</sup>	Other name	Type (NED <sup>2</sup> )	$D_{25, '}$ (LEDA <sup>3</sup> )	$M_B$ (LEDA)	$(B - V)_{3\sigma}^4$	$V_r$ , km/s (NED)	$\Delta$ , Mpc <sup>1</sup>
–	NGC 80	SA0–	1.82	–21.6	1.03	5698	$\sim 0$
029	–	–	0.36	–17.6	0.84	5709	0.117
030	–	–	0.33	–17.9	0.95	6035	0.132
034	NGC 81	–	0.41	–18.8	0.99	6130	0.097
035	–	–	0.33 <sup>4</sup>	–18 <sup>4</sup>	0.96	5372	0.111
040	NGC 85	S0	0.68	–19.5	1.18	6204	0.115
016	IC 1541	S0	0.72	–19.4	1.04	5926	0.544
055	IC 1548	S0	0.68	–19.3	1.00	5746	0.400
058	NGC 93	S (Sb <sup>3</sup> )	1.32	–20.8	1.06	5380	0.096
041	NGC 86	Sbc (S0/a <sup>3</sup> )	0.74	–20.0	1.05	5591	0.153
044	MCG +04 – 02 – 010	S (Sbc <sup>3</sup> )	0.89	–20.3	1.17	6630	0.185
051	CGCG 479-014B	Sc	0.63	–18.5	0.93	5850	0.377
–	UCM 0018+2216	Sb	0.29	–17.3	0.72	5066	0.14

<sup>1</sup>Mahdavi & Geller (2004); the distance of 77 Mpc is taken from this paper as well<sup>2</sup>NASA/IPAC Extragalactic Database<sup>3</sup>Lyon-Meudon Extragalactic Database<sup>4</sup>This work

Here we study the structure of lenticular galaxies, as well as early-type spiral galaxies, which are the most likely candidates for precursors of S0 galaxies, all the members of the massive X-ray group of NGC 80. This group is also known as GH3 [14], SRGb063 [15], and U013 [16], and is sometimes classified as a poor cluster (WBL 009) [17]. The X-ray flux from the NGC 80 group is  $\lg L_X(h_{100}^{-2}, \text{erg/s}) = 42.56 \pm 0.09$  [15], which is typical for rich groups, and its total mass estimated from the X-ray luminosity exceeds  $10^{14} M_\odot$  [16]. The group extends over a degree (more than 1 Mpc) on the sky plane. Redshift measurements were used to select 45 group members in [18]; our visual inspection of the images indicates that at least half of these (24 galaxies) are late-type spiral galaxies, which is unexpected, given the powerful X-ray halo of the group. Could it be that the group of NGC 80 is a young group, so that the process of transforming spiral members into lenticular ones has not yet finished? To investigate the properties of a sample of lenticular galaxies in this group, we have obtained CCD-images in the  $B$  and  $V$  bands for six-arcminutes fields around five large galaxies studied by us earlier in [19], and have carried out surface photometry of the targets with dimensions exceeding  $10''$ . A list of galaxies studied is given in Table 1 together with their global (literature) characteristics.

## 2 OBSERVATIONS

The photometric data were obtained at the 6-m telescope of the Special Astrophysical Observatory of the Russian Academy of Sciences with the SCORPIO [20] in a direct-image mode. The detector was a  $2048 \times 2048$  EEV 42-40 CCD. The exposures have been acquired under double binning that provided a scale of  $0.35''$  per pixel. The field of view was  $6.1'$ . The observations have been carried out in the standard Johnson  $B$  and  $V$  bands. An exposure of twilight sky was used as a flat field.

A detailed list of observations is given in Table 2. The observations of the group of NGC 80 were undertaken on August 21, 2007, under photometric conditions, and the seeing was about  $2''$ . We took exposures of five

Table 2: Photometric and spectral observations of the group galaxies in 2007-2008.

NGC/IC	Observation date	Instrument/mode	Spectral range	Exposure time, s	Seeing
80	21.08.2007	SCORPIO/IMAGER	<i>V</i>	60	2.3''
80	21.08.2007	SCORPIO/IMAGER	<i>B</i>	180	2.1''
93	21.08.2007	SCORPIO/IMAGER	<i>B</i>	180 × 2	2.0''
93	21.08.2007	SCORPIO/IMAGER	<i>V</i>	60 × 3	2.0''
86	21.08.2007	SCORPIO/IMAGER	<i>V</i>	120 × 2	2.2''
86	21.08.2007	SCORPIO/IMAGER	<i>B</i>	180 × 3	2.0''
1548	21.08.2007	SCORPIO/IMAGER	<i>V</i>	120 × 2	1.9''
1548	21.08.2007	SCORPIO/IMAGER	<i>B</i>	180 × 3	2.1''
1541	21.08.2007	SCORPIO/IMAGER	<i>B</i>	180 × 3	1.8''
1541	21.08.2007	SCORPIO/IMAGER	<i>V</i>	90 × 3	2.3''
85	04.09.2008	MPFS	4200–5600 Å	5400	1.9''
1541	02.09.2008	SCORPIO/Long-Slit	5700–7000 Å	1800	2.3''

fields centered onto the most luminous galaxies of the group, NGC 80, NGC 86, NGC 93, IC 1548, and IC 1541. The central galaxy NGC 80 was used as a photometric standard: a good collection of aperture photoelectric photometry is available for this galaxy in the HYPERLEDA database, mainly from [21].

In addition to the photometric data, we have analyzed some spectral observations. The central part of NGC 85 was observed with the MPFS (Multi-Pupil Fiber Spectrograph) integral-field unit of the 6-m telescope in September 2008 in the blue-green spectral range, 4150–5650 Å, with a reciprocal dispersion of 0.75 Å per pixel (and a spectral resolution of about 3 Å) (for a description of this instrument, see [22]). The detector for these observations was the same 2048 × 2048 CCD array. In the MPFS, a 16 × 16 microlens array provides a pupil set, which are connected to the entrance of the long-slit spectrograph. Such configuration enables the simultaneous registration of 256 spectra, each of which corresponds to a spatial element of the galaxy image 1'' × 1'' in size; accordingly, the MPFS field of view is 16'' × 16''. The MPFS data were used to investigate the rotation of the stellar component in the center of NGC 85 (we were not able to detect emission lines in the galaxy), through a cross correlation with the spectra of K giant stars observed on the same night with the same spectrograph. The age and metallicity of the stellar population in the nucleus and circumnuclear region have been estimated by calculating the Lick indices H $\beta$ , Mgb, Fe5270, and Fe5335 [23] and by comparing them to the models for "simple stellar populations" (SSP) by Thomas et al. [24].

To study the kinematics at distances of more than 8'' from the center, the lenticular galaxy IC 1541 which is located at the periphery of the group was observed on September 2, 2008 with the SCORPIO reducer in a long-slit mode. The slit orientation was close to the major axis of the galaxy. The exposure was 30 min, and the red grism was used as a disperser, providing a spectral range of 5700–7400 Å and a spectral resolution of about 5 Å. The original aim was to search for weak emission lines, H $\alpha$  or [NII] $\lambda$ 6583, from the ionized gas in IC 1541. However, no traces of emission were detected, and the data were instead used to estimate stellar line-of-sight velocities along the major axis (a rotation curve) via cross correlation of the galaxy spectra at various distances

from the center with the spectra of twilight sky taken on the same night with the same instrumentation.

### 3 ANALYSIS OF THE STRUCTURE FOR THE DISK GALAXIES IN THE NGC 80 GROUP

We have carried out decomposition of the  $B$  and  $V$  radial surface brightness profiles of the galaxies under consideration. Figures 1 and 2 show the original  $V$  images of the galaxies, together with the residual brightnesses after subtracting the models.

The decomposition was carried out by using the interactive GIDRA program, which successively constructs one-dimensional profiles and two-dimensional models (for the description of its application see [25]). The whole procedure starts from constructing radial profiles of the surface brightness averaged in elliptical rings. The shape of these elliptical rings (position angles, major axes, and axial ratios) is specified based on isophotal analysis of the images made with the program FITELL from V.V. Vlasyuk. Images of foreground stars projected against the galaxies were either masked or removed by subtracting a symmetrical profile corresponding to the scattering function for a point source (the case of a bright star next to NGC 86). Further, having constructed the azimuthally averaged surface-brightness profiles, the GIDRA program fits it with a Sersic law [26]:

$$\mu(r) = \mu_e + 1.086b_n[(r/r_e)^{\frac{1}{n}} - 1],$$

where  $n$ ,  $r_e$ , and  $\mu_e$  are parameters of the model and the coefficient  $b_n \approx 2n - 0.32$ . We separate structural components of a galaxy, starting with the outer regions which we assume to be exponential disks [27] – a particular case of a Sersic law with  $n = 1$ . Having fitted an exponential to the brightness profile of the outer stellar disk and determined its parameters, we construct a two-dimensional model (image) of this disk and subtract it from the observed galaxy image. After that, the procedure of constructing and fitting an azimuthally averaged surface brightness profile is repeated once more. If the ellipticity of the residual isophotes is not very different from the ellipticity of the outer isophotes, we conclude that a separate inner stellar disk is present in the galaxy, and fit it using an exponential law with new parameters. After subtracting the inner disk, there usually remained a central bulge, for which the Sersic parameter  $n$  was set free. However, in the most cases, we obtained an exponential brightness profile for the bulges as well. This is the first conclusion of our analysis of the structure of the early-type disk galaxies in the NGC 80 group: most of them have exponential bulges and two-tiered exponential disks. An example of decomposing the brightness profile for a giant lenticular galaxy (IC 1541 at the periphery of the group) into two disks and an exponential bulge is shown in Fig. 3a. This galaxy is seen nearly edge-on, and a boxy central structure associated with the bulge is visible in the the galaxy; outside the bulge, the two stellar disks with different exponential scales have comparable thicknesses. Figure 3a demonstrates how deep our photometry is: the galactic disk extends to a radius of 30 kpc, and the

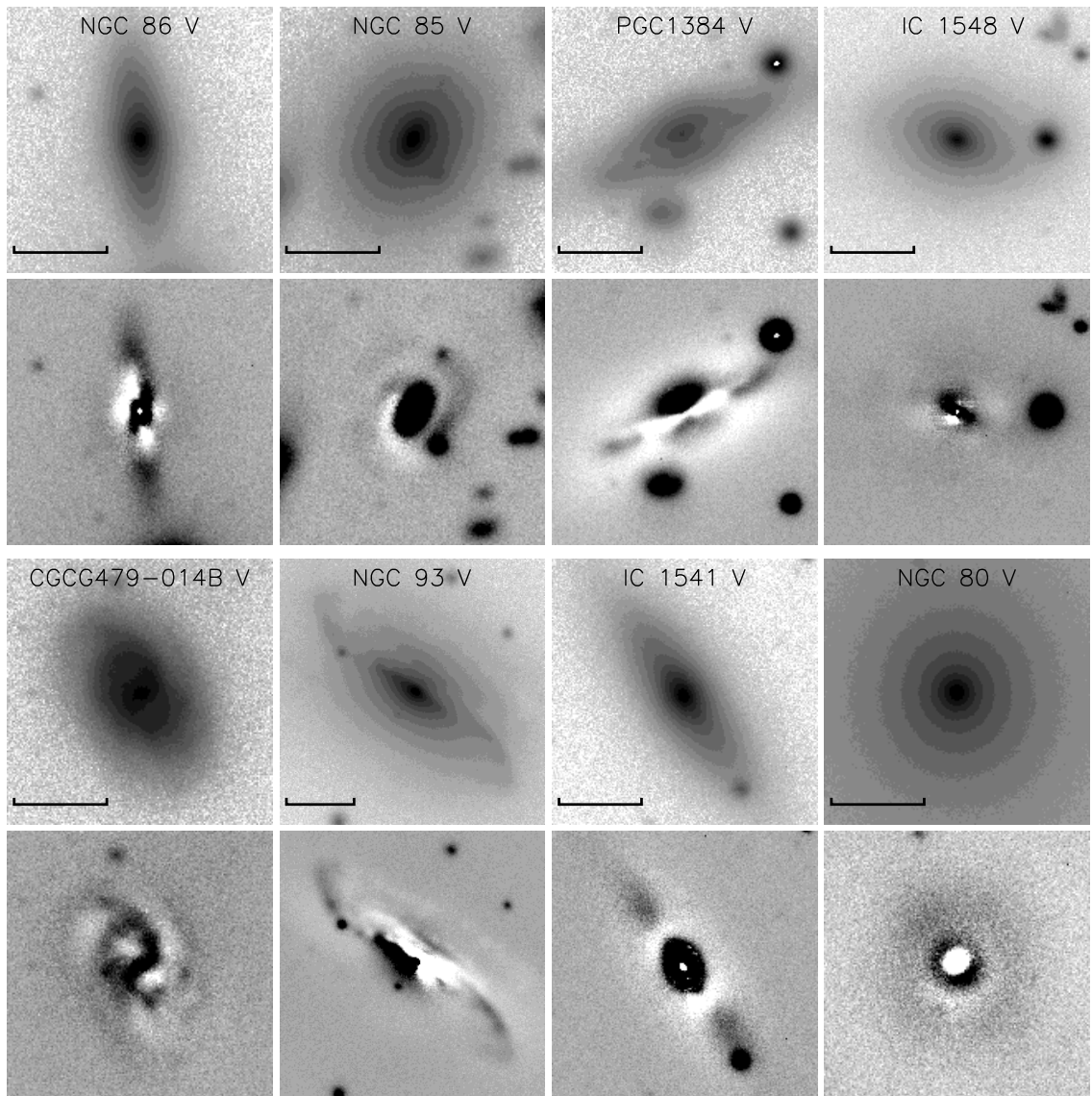


Figure 1:

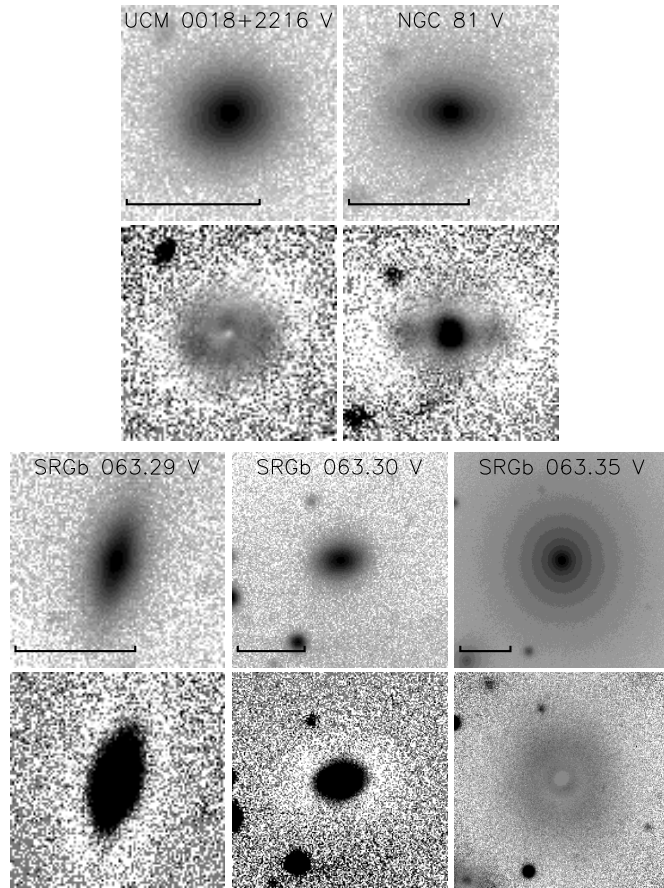


Figure 1:

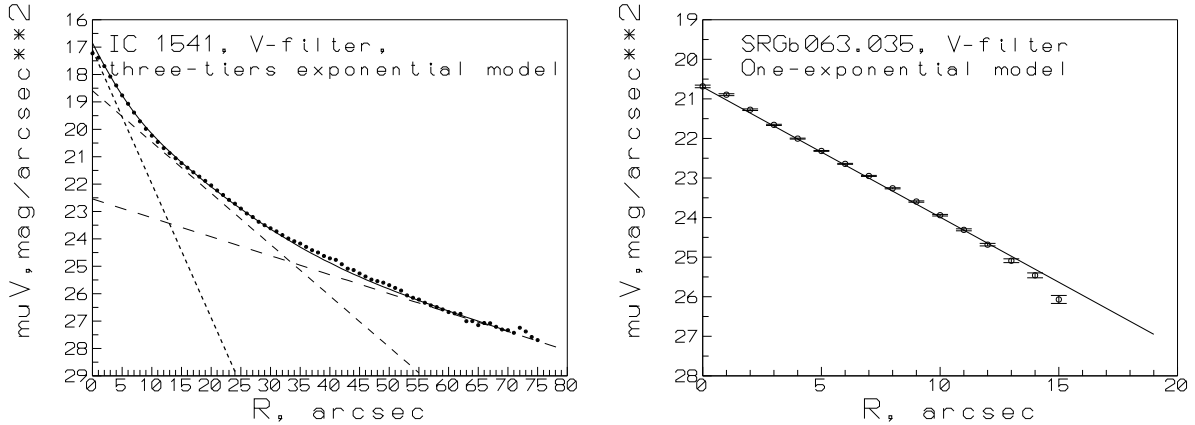


Figure 3: Examples of decomposing the surface brightness profiles into components. *a* – The giant lenticular galaxy IC 1541. The long-dashed line is an outer disk model, the short-dashed line is an inner disk model, and the dotted line shows the model of a pseudobulge. The points represent the observational  $V$ -brightness profile azimuthally averaged along the ellipses with parameters derived from the isophotal analysis. The solid curve gives the final fit by a sum of model components. *b* – The dwarf galaxy SRGb 063.035 – the nearest companion to NGC 80. The total profile is perfectly fitted by a single exponential law.

surface brightness limit is  $\mu_V = 27.7^m / \text{arcsec}^2$  being well beyond the Holmberg radius.

The parameters of the photometric models for the sample galaxies are presented in Table 3, which gives the central surface brightness  $\mu_0 = \mu(0)$ , *not* reduced to a face-on orientation. All the luminous lenticular galaxies have two-tiered exponential disks and exponential bulges. The bulge of the giant spiral NGC 93 is well fitted with a Sersic parameter of two, that is typical for giant Sb galaxies. An interesting feature is found in the dwarf lenticular galaxies which are satellites of NGC 80 – the central galaxy of the group: three of four display a single-scaled stellar disk, and, when present, the central spheroid is best-fitted with a Sersic law with the index  $n < 1$ , that is typical for dwarf diffuse spheroidal galaxies. In one case – namely in the nearest close companion to NGC 80, SRGb063.035 – there is no bulge at all, and the whole galaxy consists of a single exponential disk (Fig. 3b). A structure with very low surface brightness is also visible around the single exponential disk of a close companion to NGC 86 – UCM 0018+2216, which is classified as a Sb galaxy according to the NED. However, no spiral arms are seen in the disk of UCM 0018+2216 in our plots, both  $B$  and  $V$ , and we re-classify it as a S0 galaxy that is probably in the process of forming. It is obvious that the tidal influence of massive neighbors truncates the brightness profiles of the dwarf galaxies and stimulated their secular evolution, smoothing the whole stellar density profile into a single exponential law. This provides an interesting hint to possible origins of the exponential shapes of surface brightness profiles of stellar disks which are not understood yet.

Figure 4 compares the central surface brightnesses and scalelengths for the exponentials fitted to all three types of structural components – the outer and inner disks and the exponential bulges. The central surface brightnesses reduced to face-on orientation are plotted; we necessarily took into account the internal absorption in the galaxies, as well as the fact that stellar disks in the lenticular galaxies are thick. Historically, after the publication of the first statistics of the stellar disk parameters for nearby galaxies by Freeman [27], who reported



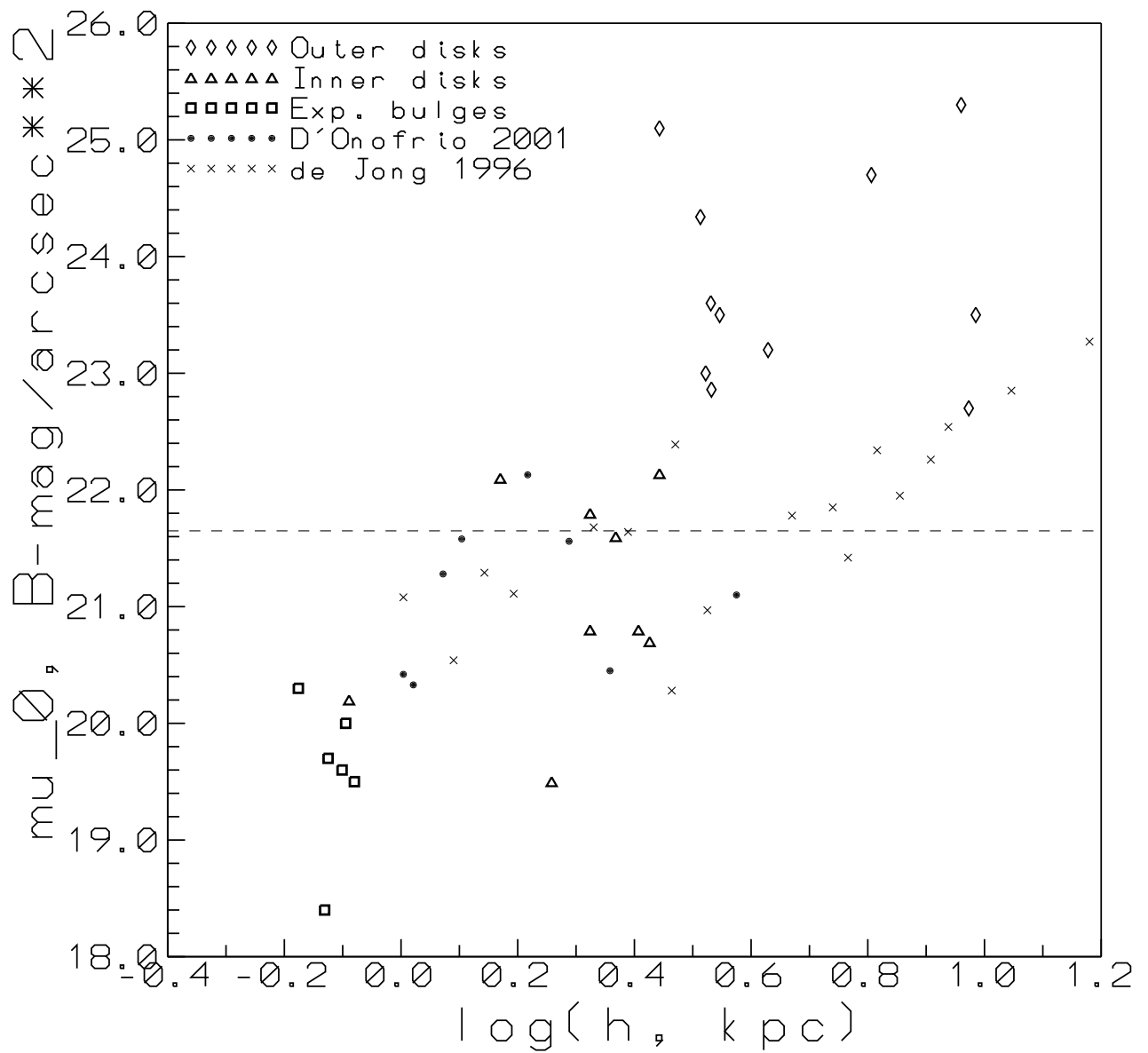


Figure 4: Empirical relation between the central surface brightnesses and the exponential scalelengths for stellar disks of early-type galaxies. The results of our decomposition – the outer disks, the inner disks, and the pseudobulges – are plotted together with the literature data obtained within the framework of the one-exponential disk model. The horizontal dashed line indicates the mean central surface brightness of nearby luminous stellar disks by Freeman (1970).

Table 3: Parameters of the photometric components of the galaxies in the group NGC 80

Galaxy	Band	$PA^1$	$(1 - b/a)^1$	Outer disk			Inner disk			$n$	Bulge		
				$\mu_0, m/arcsec^2$	$h''$	$h, kpc$	$\mu_0, m/arcsec^2$	$h''$	$h, kpc$		$\mu_0, m/arcsec^2$	$h''$	$h, kpc$
(NGC)80	<i>B</i>	$4^\circ$	0.11	22.6	25.1	9.4	20.7	5.7	2.1	1	18.4	2.0	0.7
(NGC)80	<i>V</i>			21.4	27.7	10.3	19.4	4.8	1.8	1	17.3	1.8	0.7
(SRG)29	<i>B</i>	$166^\circ$	0.52	24.1	8.8	3.3	—	—	—	—	—	—	—
(SRG)29	<i>V</i>			23.1	8.7	3.2	—	—	—	—	—	—	—
30	<i>B</i>	$100^\circ$	0.26	23.2	9.5	3.5	—	—	—	—	—	—	—
30	<i>V</i>			23.0	9.4	3.5	—	—	—	—	—	—	—
34	<i>B</i>	$110^\circ$	0.1	24.6	17.3	6.5	20.1	2.2	0.8	1	19.0	1.1	0.4
34	<i>V</i>			23.3	16.7	6.2	19.1	2.2	0.8	1	17.9	1.1	0.4
35	<i>B</i>	$159^\circ$	$0.1 - 0.18$	—	—	—	22.0	4.0	1.5	—	—	—	—
35	<i>V</i>			—	—	—	20.7	3.3	1.2	—	—	—	—
40	<i>B</i>	$148^\circ$	0.18	22.6	9.2	3.4	21.6	5.7	2.1	1	20.0	2.2	0.8
40	<i>V</i>			21.6	9.2	3.4	20.3	6.2	2.3	1	19.0	2.4	0.9
16	<i>B</i>	$35^\circ$	0.64	24.5	24.6	9.2	21.3	7.5	2.8	1	19.2	2.1	0.8
16	<i>V</i>			22.5	15.7	5.9	18.6	5.8	2.2	1	17.1	2.2	0.8
55	<i>B</i>	$85^\circ$	0.36	23.1	11.5	4.3	21.5	6.3	2.4	1	19.5	2.2	0.8
55	<i>V</i>			22.4	12.5	4.7	20.6	6.3	2.4	1	18.6	2.5	1.0
58	<i>B</i>	$53^\circ$	0.36	23.4	26.1	9.7	20.6	7.2	2.7	2	20.6	4.1	1.5
58	<i>V</i>			22.5	25.5	9.5	19.4	7.6	2.8	2	19.5	3.1	1.2
41	<i>B</i>	$8^\circ$	0.64	22.8	9.0	3.4	19.1	4.8	1.8	1	19.3	2.0	0.8
41	<i>V</i>			22.2	11.4	4.2	18.9	4.9	1.8	1	18.4	2.0	0.8
44	<i>V</i>	$116^\circ$	0.53	23.4	23.0	8.6	21.0	9.0	3.4	—	—	—	—
51	<i>B</i>	$32^\circ$	0.32	22.6	9.0	3.4	20.4	6.9	2.6	—	—	—	—
51	<i>V</i>			22.7	9.6	3.6	19.5	6.9	2.6	1	22.9	1.4	0.5
UCM	<i>B</i>	$105^\circ$	0.10	25.0	7.5	2.8	—	—	—	1	20.3	1.8	0.7
UCM	<i>V</i>			24.0	7.0	2.6	—	—	—	1	19.5	1.8	0.7

<sup>1</sup>Orientation parameters (major-axis  $PA$  and isophote ellipticity) relate to the outermost isophotes.

that the central surface brightnesses were grouped tightly near the value of  $\mu_0(B) = 21.7^m/arcsec^2$  and had a Gaussian distribution with the width of the order of the measurement errors, all subsequent photometric surveys gave broad distributions for the central surface brightnesses and a correlation between the central surface brightness and the exponential scalelength (see, for example, [28, 29, 30, 31]). However, these surveys did not allow for the possible presence of multi-tiered exponential disks. A correlation between the central surface brightness and the exponential scalelength is also obvious in our Fig. 4, where up to three structural components are plotted for every galaxy. However, we can now see that the origin of this correlation is due to the presence of three types of structural components with a various degree of concentration toward the center. The three clouds of points corresponding to the outer disks, inner disks, and exponential bulges have different mean scales and central surface brightnesses, but no correlation between the scalelengths and the central surface brightnesses is observed within each cloud of points. The outer disks all have lower surface brightnesses than the "Freeman's standard", while the inner disks are all near this line and brighter. We cannot rule out that there is no physical correlation between scalelength and surface brightness, but there exist several types of stellar disks of different origins. However, this conclusion waits for verification with a larger statistics of surface brightness profile decomposition taking into account the presence of multi-tiered disks.

After the construction of the model images for the galaxies studied and the subtraction of these from the observed ones, apart from the large-scale structural components, we have derived also a lot of small-scale peculiar structures which are clearly visible in the residual brightness maps in Figs. 1 and 2. Below we present a brief description of these substructures for every galaxy.

**NGC 86.** The stellar population in the galactic center is old [19]. After subtracting the outer and inner

exponential disks, a boxy bulge with spiral arms is left in the residual brightness distribution, with the position angle of the major axis of the bulge, about  $170^\circ$ , differing substantially from the orientation of the disks. The best fit to the bulge is obtained using a Sersic law with the index of one (an exponential bulge) and with  $r_0 = 2''$ ,  $\mu_0 = 19^m/arcsec^2$ , and the ratio of the minor and major axes being about 0.95. Subtracting this bulge leads to a residual image that is reminiscent of a bar that is evolved in the  $z$ -direction. The residual brightness after this subtraction occupies roughly 50% of the total area of the bulge, i.e., it is more compact. We suggest that the exponential bulge of the galaxy is a pseudobulge whose origin is associated with the development of vertical instability in a bar [32].

**NGC 85.** The outer disk starts to dominate the brightness distribution at distances  $r > 20''$ , or 7.5 kpc, from the center, and its parameters are typical for the disks of spiral galaxies (Table 3). After subtracting the outer disk, the residuals have an exponential profile with excess brightness near the southern edge. It seems that the remaining inner disk has a higher inclination and a smaller position angle than the outer disk. The new orientation parameters are  $i = 50^\circ$ ,  $PA = 137^\circ$ . Fitting an exponential to the brightness profile in the radius range of  $8'' - 15''$  yields the parameters of a second disk (Table 3). After subtracting this disk as well, the residuals resemble a small lens-like region with tails. It is interesting that the position angle of the small lens seems to be closer to the position angle of the outer disk than to that of the inner disk, whereas the opposite is true for its inclination. We have recently seen a similar structure in the lenticular galaxy with counterrotating gas NGC 5631, which clearly demonstrates signatures of minor merger [33]. Further fitting of the residual brightness profile for NGC 85 seems to indicate a fairly elongated exponential bulge ( $b/a = 0.83$ ). The residuals after subtraction of this bulge visually resemble three features with tails, which are likely a consequence of a recent merger, which also led to the formation of the lenticular galaxy.

**PGC 1384.** It is immediately obvious that this galaxy contains large amount of dust. Since the galaxy is viewed nearly edge-on, the dust strongly impedes the decomposition, as the galactic center is hidden behind this dust. It is interesting that the dust is not visible in the outer disk of this very dusty galaxy, which apparently testifies to secular evolution during which the gas and dust have become concentrated near the galactic center. Therefore, we adopted as the model center the center of the outer isophotes. The fitting of the outer disk was carried out for  $r > 30''$ . At  $r < 19''$  the residual profile in the  $V$ -band is well-fitted by an exponential law corresponding to a second disk. We are not able to analyze the most central region of the galaxy, since it is strongly contaminated by the dust, even in the  $V$ -band.

**UCM 0018+2216.** The name of this galaxy means that it has been detected in the Universidad Complutense de Madrid survey, which is aimed to search for emission-line galaxies. Subsequent long-slit spectroscopy [34] has shown that star formation of modest intensity is occurring in the galactic nucleus. Our images display a weak asymmetry of the galaxy relative to the center of the inner isophotes: its south-eastern half is more elongated than its north-western part. Because of this, the northern parts of the galaxy are slightly oversub-

tracted, and the residual brightness distribution is shifted to the south of the center. The outer disk dominates at  $r > 13''$ . After subtracting the outer disk, a second exponential disk can be fit to the residual profile at  $r = 2'' - 6''$ . After subtracting both disks, there remains an interesting region resembling a boxy bulge with an elongated shape and a kind of low-contrast, tightly wound spiral structure (a ring?) visible in the  $B$ -band.

**IC 1548.** The stellar population in the galactic center is young, younger than 1.5 Gyr in the nucleus and about 3 Gyr in the bulge [19]. After subtracting the two exponential disks from this fairly strongly inclined lenticular galaxy, there remains a circular exponential bulge surrounded by rudimentary spirals.

**CGCG 479-014B.** This is a late-type spiral with a large bar. The brightness profile of the outer disk is of type II according to the definition by Freeman [27] – exponential with a hole in the center. The bulge is small and circular, and its Sersic parameter is determined only uncertainly due to its compactness.

**NGC 93.** Our previous study [19] has revealed a chemically distinct nucleus inside the old bulge of this galaxy, which has formed 3-4 Gyr ago in a secondary burst of star formation. The powerful dust lane visible in images indicates that the north-western part of the disk is the nearest to us. When constructing our models, we had to mask both the region of strong dust absorption and the high-contrast spiral arms. The outer disk begins to dominate at  $r = 43''$  (16 kpc), while the inner disk dominates at  $r = 20'' - 40''$ . After subtracting the two disks, there remains a small lens-like region that is asymmetrical due to crossing by the dust lane. It is possible to fit the residual brightness at  $r = 5'' - 11''$  by a single ring-like disk (with a hole in its center), with its brightness profile cut off at  $r > 11''$ . After fitting the residual brightness at  $r = 2'' - 11''$  with a Sersic bulge with  $n = 2$  and isophote ellipticity of 0.75, a very interesting residual brightness distribution appears, which resembles a one-sided bar (whose other half is hidden by the dust), or a satellite that is disrupted by tidal forces.

**IC 1541.** The stellar population at the galactic center is old [19]. See Fig. 3a for an analysis of the surface-brightness profile. The apparent axial ratio for the exponential bulge is 0.8.

**NGC 80.** The decomposition results for this galaxy agree well, as concerning the scalelengths, with the results published by us previously based on less deep data [35]. The outer regions can be fit with an exponential profile from a radius of  $30''$  (11 kpc). The inner disk dominates at radii of  $10'' - 20''$  (4–7 kpc). After subtracting the two disks, the residual brightness at  $r = 2'' - 8''$  can be fit with a circular exponential bulge. Excess brightness is visible at  $r = 5'' - 7''$ , consistent with the position of a ring of relatively young stars ( $T \sim 5$  Gyr) [35, 19].

**NGC 81.** An outer exponential disk fits the galaxy profile well at  $r > 15''$ , and an inner disk – from  $r > 6''$  to  $12''$ . After subtracting these two disks, the residual structure resembles a lens with weak spiral arms, which we fit by an exponential bulge with axial ratio of  $b/a = 0.95$ . After subtracting the bulge, there remain residual tails resembling a spiral structure. The bulge has boxy isophotes.

**SRGb 063.030.** The outer disk reveals an exponential profile starting from  $r = 11''$  (4 kpc). After disk subtraction, the residual profile has a bell-like shape that cannot be fitted by a Sersic law with  $n \geq 1$ .

**SRGb 063.029.** The outer disk starts at  $r = 15''$  (5.5 kpc). After subtracting this outer disk, the residual profile has a bell-like shape.

**SRGb 063.035.** This galaxy is very compact, and can be fitted by a single exponential disk (Fig. 3b). It is most likely that its outer regions have been truncated by the tidal influence of NGC 80, which is at a distance of only 20 kpc in projection onto the sky plane.

## 4 ROTATION CURVE OF THE LENTICULAR GALAXY IC 1541

We have obtained the long-slit spectrum of IC 1541 with the SCORPIO, the slit being aligned roughly with the major axis of the galaxy. We aimed to search for ionized gas, but no signs of emission lines were detected in the long-slit spectrum over the full extent of the galactic disk. However, we have used this spectrum to estimate the rotational velocity of the stellar component: we were lucky to measure line-of-sight (LOS) stellar velocities from absorption lines to the radius of  $15''$  (6 kpc).

As we noted above, the surface brightness profile of IC 1541 can be decomposed into three exponential segments with different scalelengths. By analyzing only the surface photometry, the structure of the galaxy can be treated either as a combination of three disks, or of a two-tiered disk and a pseudobulge, or of an outer disk and a combined bulge. However, stellar dynamics of bulges and disks are different: any bulge is a dynamically hot (thick) subsystem, while a disk is a dynamically cool stellar subsystem, where ordered rotation dominates over random star motions (velocity dispersion). Then, we can diagnose the stellar exponential structures by comparing observed ordered stellar motions with predictions of a pure rotation model for a potential with a specified geometry and density distribution that is consistent with the observed surface brightness distribution. Here, we neglect possible contribution from dark matter, but, as is known from observational statistics, the dynamical influence of dark matter is negligible in the central regions of massive disk galaxies (see, for example, [36]).

We have taken the model for the rotation of an axisymmetrical flattened stellar system with an exponential profile for the projected surface density from [37]. This paper provides tabulated circular rotation curves for three values of ratio of the characteristic effective disk thickness to the characteristic effective radius (related to the exponential scalelength by the factor of 1.678): 0.05, 0.1, and 0.2. The last of these three values corresponds to a so-called thick disk, which is typical for lenticular galaxies [38, 39], and IC 1541 is a lenticular galaxy. Figure 5 presents the results of isophotal analysis for IC 1541 (in the  $V$ -band). Taking into account the fact that the radial dependence of the isophote ellipticity has reached a maximum value (plateau) by the radius of  $10'' - 15''$ , i.e. within the zone of photometric dominance of the middle exponential component (Fig. 3a), the two outer components are supposed to have comparable thicknesses, and are most likely disks. The inner exponential component could be either a disk or a bulge. Figure 6 compares the observed relative LOS velocities

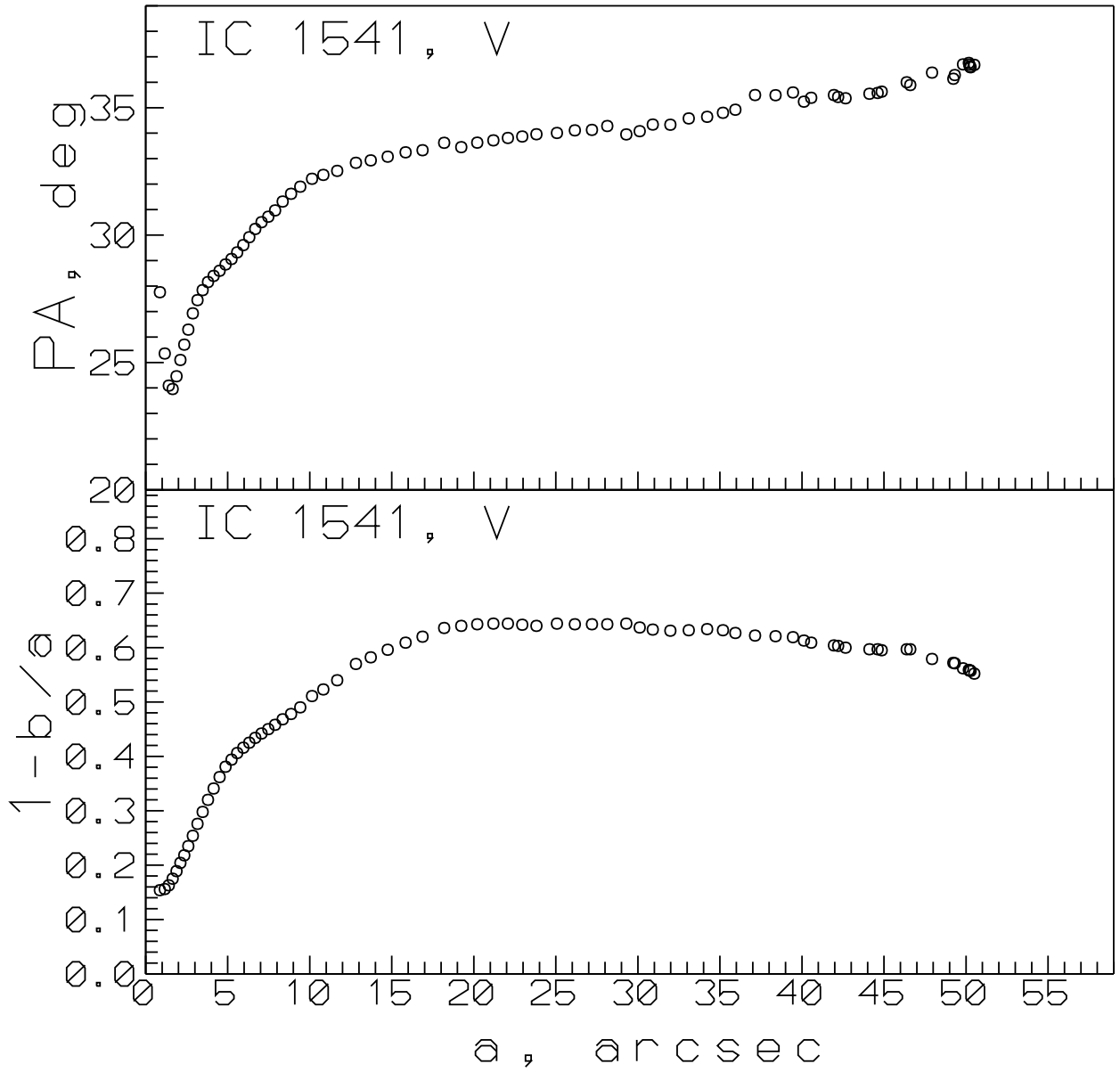


Figure 5: The results of isophotal analysis for IC 1541 (in the V-band): radial dependencies of the major axis position angle and isophote ellipticity.

for the stellar component of IC 1541 and models from [37] for two possible kinds of the middle disk – thin (the ratio of the vertical to the radial scales is 0.05) and thick (ratio of the vertical to the radial scales is 0.2); the inner exponential component is always taken as a ‘thick disk’. Based on the isophotal analysis of Fig. 5 and the guidelines given in [38], according to which for disks of finite thickness

$$\sin i = \sqrt{\frac{2e - e^2}{1 - q_0^2}},$$

where  $e \equiv (1 - b/a)$  is the apparent ellipticity of the isophotes and  $q_0$  – the true ratio of the vertical to the radial scales, we specify for the ‘thin’ disk an inclination of  $67^\circ$ , while the ‘thick’ disk is supposed to be seen edge-on. We took also  $M/L_V = 3.8$  for the mass-to-light ratio required to transform the surface brightness profile into a surface density profile, corresponding to the stellar population models of [40] for a metallicity of +0.25 and an age of 5 Gyr. Figure 6 shows that both models fit fairly the observational data for the radius range of  $5'' - 15''$  (the ‘thick disk’ model may be slightly better). Inside the radius of  $5''$ , where the innermost exponential component dominates photometrically, there is a strong discrepancy between the model and the observations. This is obviously due to the fact that the asymmetric drift has not been taken into account (the stellar velocity dispersion at the center of IC 1541 reaches 140 km/s), and also possibly because the innermost component is not a dynamically cool disk, and its relative thickness is much greater than 0.2. As expected, the influence of dark matter is not felt at the center of IC 1541.

Thus, we conclude that the innermost exponential stellar component in IC 1541 is a bulge, while the middle component is a disk with the thickness that is typical for lenticular galaxies.

## 5 MINOR MERGER OF THE LENTICULAR GALAXY NGC 85

In our previous paper [19] where the characteristics of the stellar populations in the centers of large galaxies of the NGC 80 group were derived, we suggested that the subgroup of the giant elliptical galaxy NGC 83 is currently accreting onto the NGC 80 group. We were inspired by two facts: the large difference in the radial velocities of NGC 83 and the dynamical center of the group (near to which it is projected),  $\sim 500$  km/s, and the ongoing star formation in the center of this giant elliptical galaxy. Further studies whose results we are publishing now have supported our earlier suspicions about this.

Figure 7 shows a histogram of the distribution of galactic redshifts in the area of the NGC 80 group (taken mainly from [18]) for 45 objects within  $\pm 1000$  km/s and within 1.5 Mpc from the center of the group. Although this distribution can formally be fit with a single Gaussian corresponding to a velocity dispersion of 300 km/s, which is normal for massive X-ray galaxy groups, there is a concentration of  $\sim 10$  objects near the redshift of NGC 83 ( $v_r \approx 6200$  km/s). Excluding these objects from the NGC 80 group reduces the estimate of the galaxy velocity dispersion to 224 km/s. The histogram in Fig. 7 on its own does not enable us to extract the

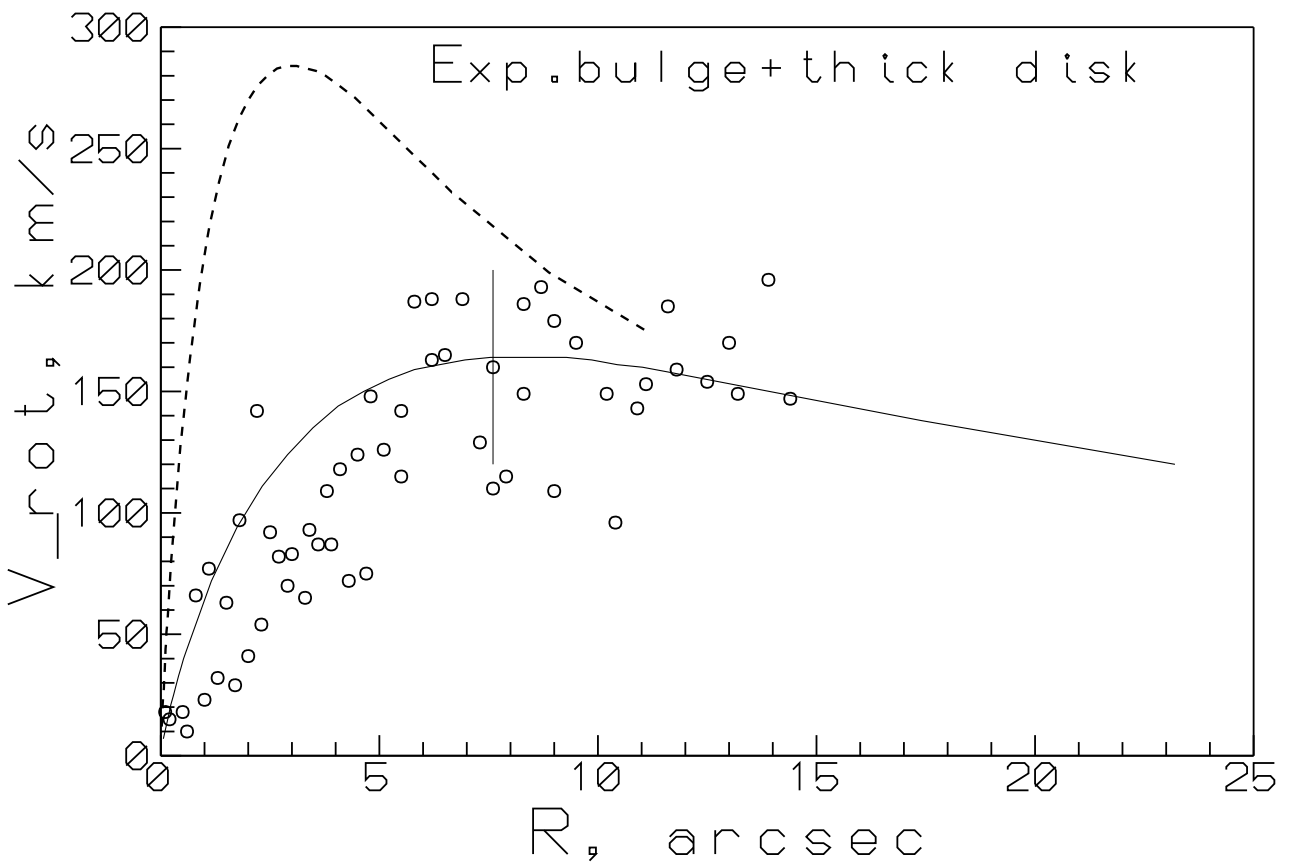
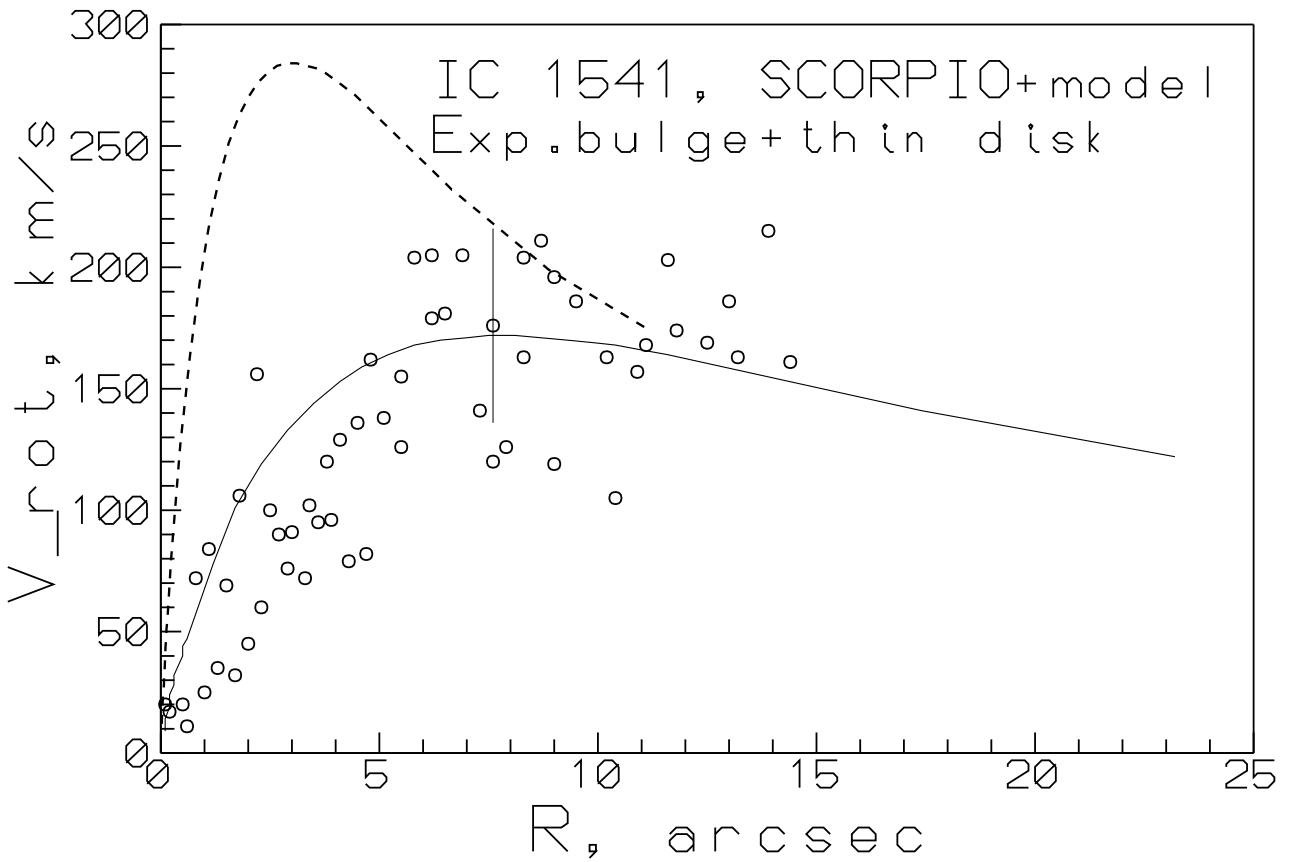


Figure 6: Rotation curve for the stellar component of IC 1541. The circles present the observational data (the SCORPIO), the solid curve is the dynamical model for the inner disk (the middle exponential component with parameters derived from the surface photometry, under two assumptions about the disk thickness, see the text for details), and the dashed curve shows the dynamical model for the most central exponential component



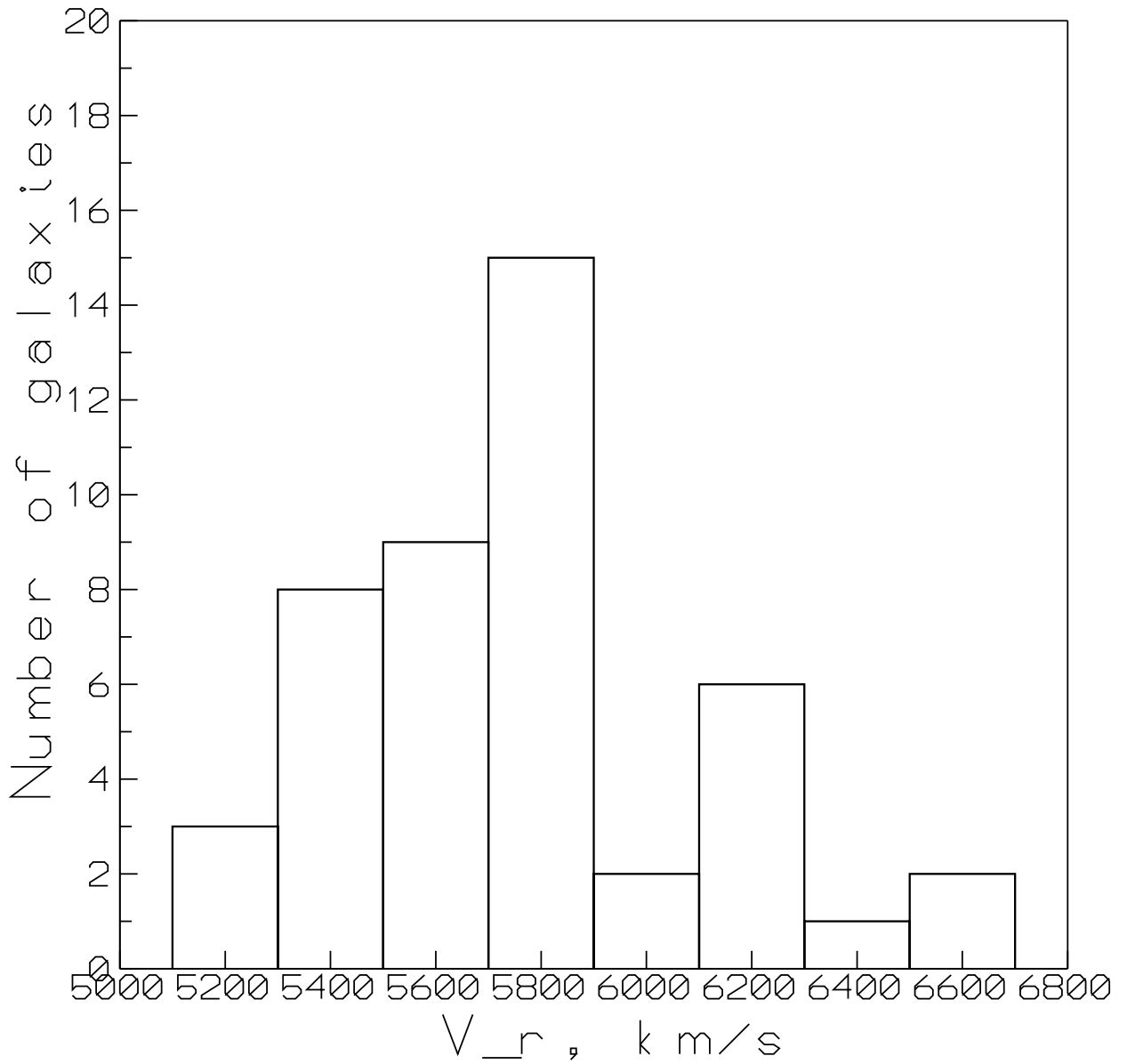


Figure 7: Histogram of the distribution of galaxy redshifts in the NGC 80 group according to the data of [18]. The systemic velocity of the group and the velocity of the central galaxy, NGC 80, are about 5700 km/s.

NGC 83 subgroup in a statistically significant way; however, we can note certain common properties of the galaxies concentrated near the redshift of NGC 83. First, these are also concentrated spatially around NGC 83: most of them are located to the North of the group center (NGC 80). Second, almost all of these galaxies display ongoing or recent star formation, including NGC 83 itself which is a giant elliptical. In addition to NGC 83, SRG 063.023 is a Markarian galaxy (Mrk 1142) indicating that its nucleus has ultraviolet excess in the spectrum. The giant spiral galaxy MGC +04 – 02 – 010 is detected in the Madrid survey of emission-line galaxies as UCM 0018+2218 [41], and it is spectrally classified as a starburst galaxy (SBN) in [34]. Finally, the lenticular galaxy NGC 85, which is located near NGC 83 in terms of both its velocity and its position on the sky plane, and which has been studied by us with the MPFS spectrograph, also proves to be unusually young.

Figure 8 presents a diagnostic diagram confronting the Lick indices  $H\beta$  and  $[MgFe] \equiv \sqrt{Mgb\langle Fe \rangle}$  for the galaxies NGC 83 and NGC 85 (the data from the MPFS) and models of SSP by Thomas et al. [24]. This comparison can be used to separate the effects of age and metallicity, and to determine mean values of both these characteristics for a stellar population (weighted with star luminosity). The diagram in Fig. 8 demonstrates that, very likely to NGC 83, NGC 85 has fairly young stars at its center, whose mean ages are about 1 to 2 Gyrs in the nucleus and in a ring with the radius of  $5'' - 6''$ . Obviously, the epochs of the star formation bursts in the centers of NGC 85 and NGC 83 are close, supporting the idea that these two galaxies share a common fate and are both intruders into the NGC 80 group. Opposite to NGC 83, NGC 85 contains no nuclear ionized gas, indicating that star formation has already ceased in its center. We can identify a likely provoker for this star formation burst: a close inspection indicates that the galaxy is interacting. The residual brightness distribution (Fig. 1) reveals spiral arms, which morphology is consistent with a tidal origin: one long and the opposite one short. Which of the neighbors could be the perturber? To the east of NGC 85 there is a large spiral galaxy, IC 1546, but the difference of their LOS velocities is 300 km/s, and such a fast passage would not be able to develop tidal structures. A dense, round spheroidal companion is visible to the south of NGC 85; could this be the galaxy pulling out the arms from its neighbor? Our analysis of the distribution of the  $B - V$  color for the residual brightness field (Fig. 9) disproves this hypothesis: the compact object to the south of NGC 85 has an anomalously red color to be a nearby galaxy,  $B - V = 1.4$ , and is most likely a background galaxy. However, a dense condensation at the end of the long tidal arm has an appropriate color,  $B - V = 1.1$ . This appears to be a half-disrupted satellite of NGC 85, whose accretion onto the latter has given birth to the observed tidal arms. So the lenticular galaxy NGC 85 has recently suffered a minor merger, which has probably also provoked the nuclear burst of star formation. The bases of the tidal arms are very blue,  $(B - V) \approx 0.6$ , and it is not ruled out that star formation is ongoing in the ring. If so, this indicates that there was quite recently a large amount of gas in the extended disk of the galaxy, consistent with the possibility that NGC 85, now a lenticular galaxy, was recently a spiral. We conclude that we are observing in real time the birth of a lenticular galaxy from a spiral, and, although this is occurring within the X-ray halo of the group, the mechanism forming the S0 galaxy

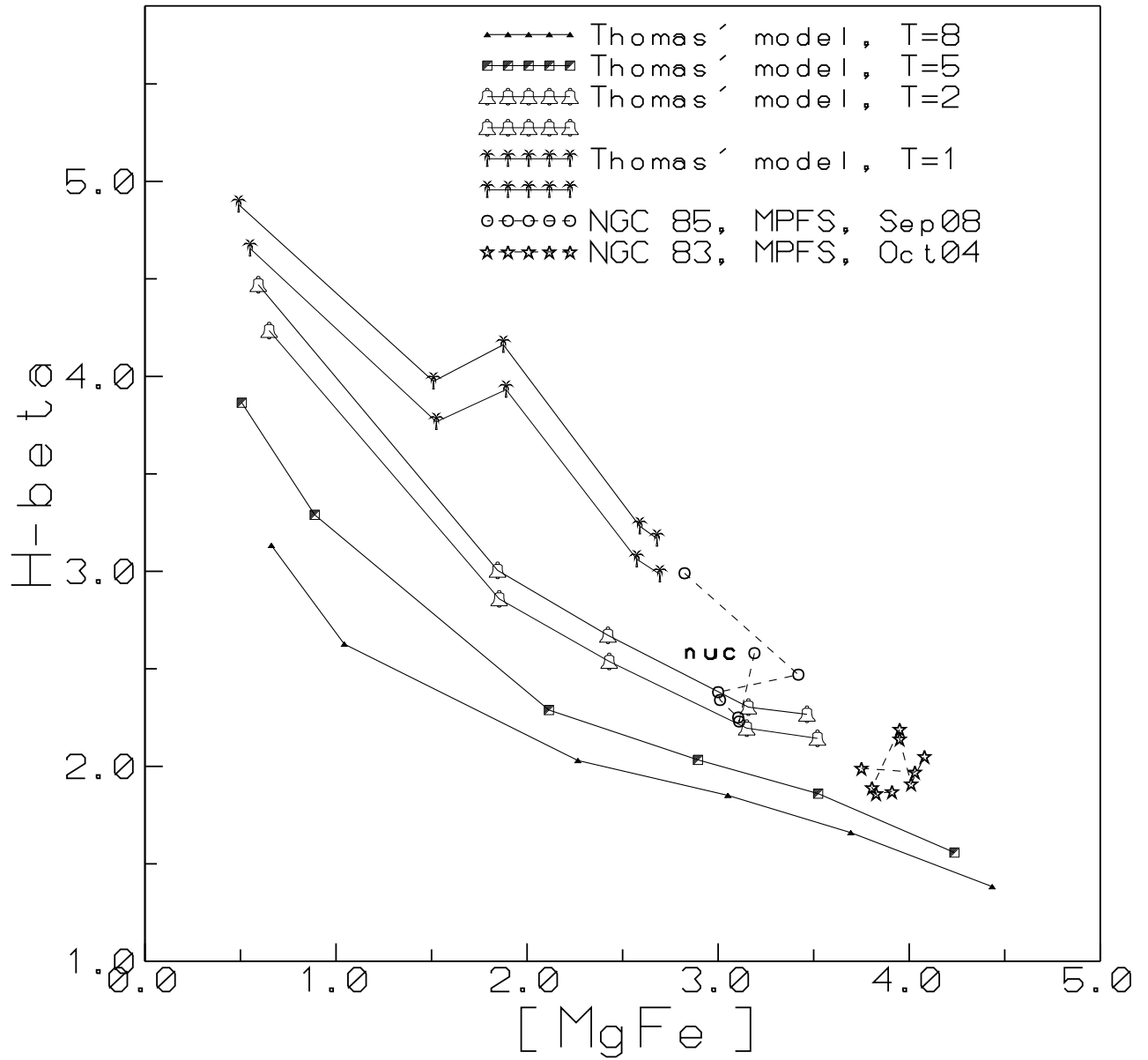


Figure 8: Diagnostic ‘index–index’ diagram for the azimuthally-averaged index measurements in NGC 85 (circles) and NGC 83 (stars). The measurements are made with the step of  $1''$  along the radii, are connected by the dashed lines; the nucleus of NGC 85 is marked by **nuc**. The model sequences of constant ages from Thomas et al. (2003) for two values of the ratio  $[Mg/Fe]$ , 0.0 and +0.3, are also plotted; the total metallicities of the models are +0.67, +0.35, 0.00, -0.33, -1.35, -2.25, if one takes the small signs along the sequences from the right to the left.

is, in this case, clearly gravitational and not gasdynamical.

## 6 CONCLUSIONS AND DISCUSSION

According to the latest views, lenticular galaxies form from spirals and are shaped completely in small groups, subsequently infalling with their groups into clusters where they are currently the dominant galaxy population (see, for example, [3]). However, the specific mechanism of this transformation has not been clear yet: many possible physical mechanisms are capable on a time scale of only one to four billion years to remove gas from the disk of a spiral galaxy, to put an end to star formation, and to heat dynamically the disk, thereby suppressing spiral structure. These can be divided into gravitational mechanisms including interactions, harassment, minor mergers and so on, and gasdynamical mechanisms acting through the interaction of cool gas of the galactic disk with hot intergalactic medium. The properties of the NGC 80 group, which is massive, rich, and possesses a hot X-ray gaseous halo, make it an ideal place for the formation of lenticular galaxies through any plausible transformation mechanism. Indeed, a close inspection of the group reveals a substantial number of lenticular galaxies: although rich X-ray groups are thought to be primarily populated by early-type galaxies, there are only three elliptical galaxies among the several dozen members, and in one of these ellipticals, NGC 83, we found earlier a massive disk and noticeable current star formation [19]. In the current study, we have investigated the structures of 13 galaxies selected among the most luminous group members. According to their NED classifications (Table 1), four of these are lenticulars, and other have later types; however, a close examination of the fine structure of their stellar disks suggests that nine are actually lenticulars (or at least non-spiral).

Our decomposition of the radial surface brightness profiles into components has shown that most of the lenticular galaxies in the NGC 80 group have two-tiered, or ‘anti-truncated’ stellar disks and compact bulges, almost all with exponential brightness profiles (which are now usually referred to as pseudobulges). This type of structure is characteristic of both galaxies near the center of the group, including the central giant S0-galaxy NGC 80, and galaxies at the periphery, projected at more than 0.5 Mpc from the group center. We do not see either any systematic variations in the structure of the disk galaxies from the periphery to the center of the group, which would have suggested the transformation of spirals into lenticulars in the course of their accretion onto the group, nor any morphological evolution due to sinking into the hot X-ray gaseous halo. The only environmental effect for which there is evidence is that four dwarf S0 galaxies ( $M_B > -18$ ) with single-scale, pure exponential stellar disks are close companions to the giant galaxies NGC 80 and NGC 86. Thus, it appears that the ‘classical’ structure of a lenticular galaxy, with a single-scale exponential stellar disk, may be obtained as a consequence of the tidal stripping of the outer parts of harassed galaxies.

One of our large lenticular galaxies, NGC 85, shows signatures of recent stimulated nuclear star formation: the mean age of the stars in its center is about one or two Gyr, and subtracting a model for the outer stellar

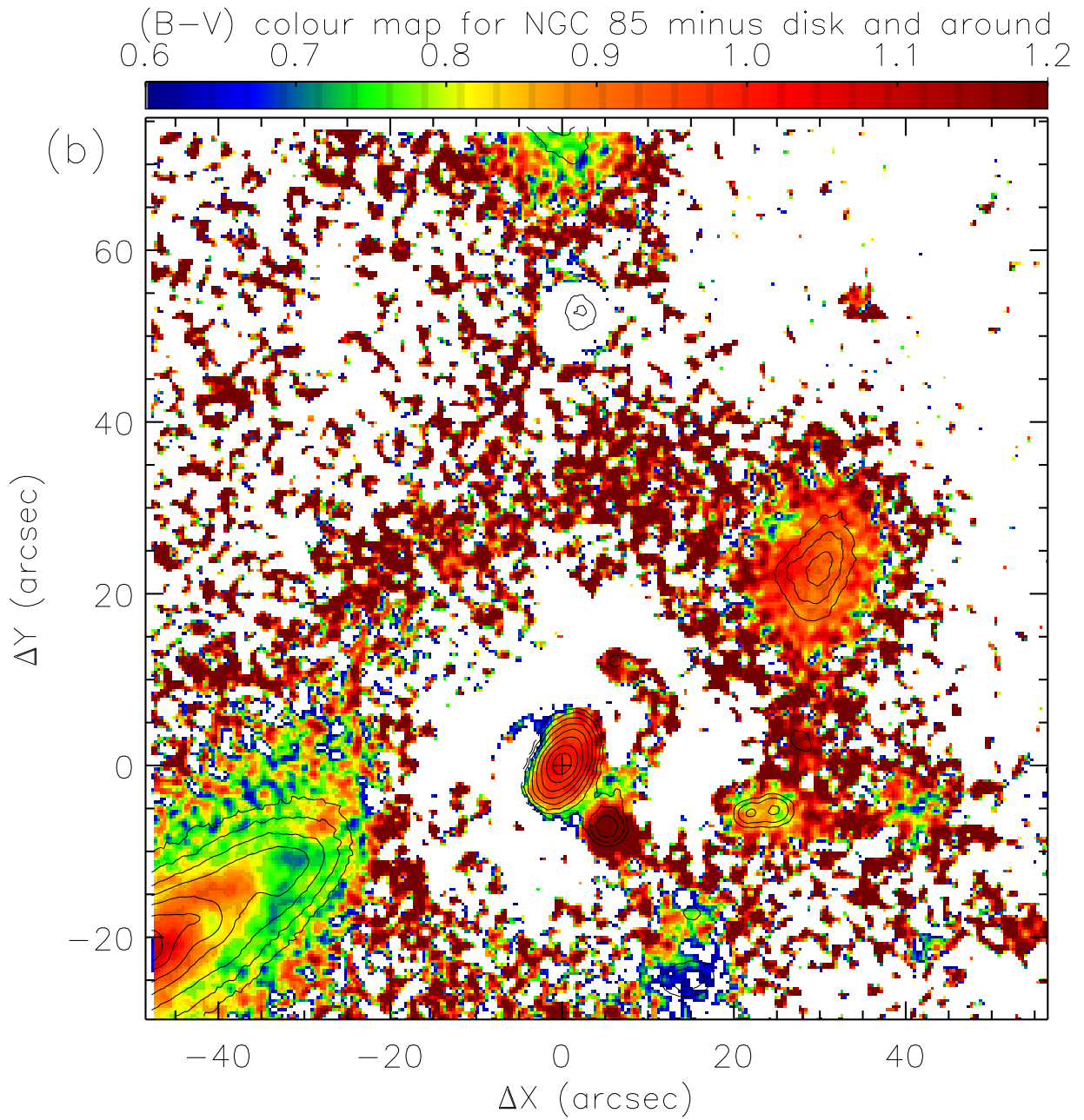


Figure 9: Map of  $(B - V)$  color for the part of the group around the galaxy NGC 85 after subtracting the outer disk of NGC 85. The isophotes show the residual  $V$ -surface brightness.

disk reveals the presence of spiral arms with blue bases that are clearly tidal in origin. It is possible that we are observing here the recent transformation of a spiral into a lenticular galaxy, accompanied by the star formation burst in the galactic center. NGC 85 is located not far from the center of the group, but, according to its radial velocity, it is associated with NGC 83, and apparently has joined the NGC 80 group only recently, together with NGC 83. The remnants of another, small galaxy can be seen at the end of a long tidal arm giving evidence for a minor merging. All this supports the idea that the mechanism for the transformation of spirals into lenticulars could be gravitational, and in particular, minor mergers would be especially effective. The properties of NGC 85 and the presence of well-formed lenticular galaxies such as IC 1541 [19], IC 1548 [19], and NGC 94 [42] at the group periphery, outside the X-ray halo, seem to be strong arguments for the dominant mechanisms responsible for the transformation of spirals into lenticulars in groups to be gravitational ones, rather than gasdynamical interaction with hot, intergalactic gas.

## 7 ACKNOWLEDGMENTS

The data analyzed here were obtained on the 6-m telescope of the Special Astrophysical Observatory of the Russian Academy of Sciences, which is supported by the Ministry of Education and Science of the Russian Federation (registration number 01-43). We thank A.A. Smirnova for supervising the MPFS observations. Our analysis made use of the Lyon-Meudon Extragalactic Database (LEDA), which is maintained by the LEDA team at the Lyon Observatory CRAL (France), and the NASA/IPAC Extragalactic Database (NED), which is managed by the Jet Propulsion Laboratory of the California Institute of Technology by contract to the NASA (USA). This work was supported by the Russian Foundation for Basic Research (project no. 07-02-00229a).

## References

- [1] Hubble E. "Realm of the Nebula". New Haven: Yale Univ. Press (1936)
- [2] Fasano G., Poggianti B.M., Couch W.J., et al. *Astrophys. J.* **542**, 673 (2000)
- [3] Wilman D.J., Oemler A., Jr., Mulchaey J.S., et al. *Astrophys. J.* **692**, 298 (2009)
- [4] Burstein D. *Astrophys. J.* **234**, 435 (1979)
- [5] Möllenhoff C., Heidt J. *Astron. Astrophys.* **368**, 16 (2001)
- [6] Quilis V., Moore B., Bower R. *Science* **288**, 1617 (2000)
- [7] Zasov A.V. *Pis'ma v AZh* **4**, 487 (1978)
- [8] Byrd G., Valtonen M. *Astrophys. J.* **350**, 89 (1990)

- [9] Moore B., Katz N., Lake G., et al. *Nature* **379**, 613 (1996)
- [10] Moore B., Lake G., Quinn T., Stadel J. *MNRAS* **304**, 465 (1999)
- [11] Oemler A. *Astrophys. J.* **194**, 1 (1974)
- [12] Dressler A. *Astrophys. J.* **236**, 351 (1980)
- [13] Butcher H.R. & Oemler A. *Astrophys. J.* **226**, 559 (1978)
- [14] Geller M.J., Huchra J.P. *Astrophys. J. Suppl. Ser.* **52**, 61 (1983)
- [15] Mahdavi A., Bohringer H., Geller M.J., Ramella M. *Astrophys. J.* **534**, 114 (2000)
- [16] Ramella M., Geller M.J., Pisani A., da Costa L.N. *Astron. J.* **123**, 2976 (2002)
- [17] White R.A., Bliton M., Bhavsar S.P., et al. *Astron. J.* **118**, 2014 (1999)
- [18] Mahdavi A., Geller M.J. *Astrophys. J.* **607**, 202 (2004)
- [19] Sil'chenko O.K., Afanasiev V.L. *Astronomy Reports* **52**, 875 (2008)
- [20] Afanasiev V.L., Moiseev A.V. *Astron. Letters* **31**, 194 (2005)]
- [21] Poulain P. *Astron. Astrophys. Suppl. Ser.* **72**, 215 (1988)
- [22] Afanasiev V.L., Dodonov S.N., Moiseev A.V.// Proc. of the Conf. "Stellar dynamics: from classic to modern", St. Petersburg, 2001/ Eds. Osipkov L.P. and Nikiforov I.I., Saint Petersburg Univ. press, p.103
- [23] Worthey G., Faber S.M., González J.J., Burstein D. *Astrophys. J. Suppl. Ser.* **94**, 687 (1994)
- [24] Thomas D., Maraston C., Bender R. *MNRAS* **339**, 897 (2003)
- [25] Moiseev A.V., Valdés J.R., Chavushyan V.H. *Astron. Astrophys.*, **421**, 433 (2004)
- [26] Sérsic J.L. *Atlas de Galaxies Australes*. Cordoba: Observatorio Astronomico (1969)
- [27] Freeman K.C. *Astrophys. J.* **160**, 767 (1970)
- [28] de Jong R.S. *Astron. Astrophys.* **313**, 45 (1996)
- [29] Iodice E., D'Onofrio M., Capaccioli M. *Astrophys. and Space Science* **276**, 869 (2001)
- [30] Graham A.W., de Blok W.J.G. *Astrophys. J.* **556**, 177 (2001)
- [31] D'Onofrio M. *MNRAS* **326**, 1517 (2001)
- [32] Bureau M., Aronica G., Athanassoula E., et al. *MNRAS* **370**, 753 (2006)

- [33] Sil'chenko O.K., Moiseev A.V., Afanasiev V.L. *Astrophys. J.* **694**, 1550 (2009)
- [34] Gallego J., Zamorano J., Rego M., et al. *Astron. Astrophys. Suppl. Ser.* **120**, 323 (1996)
- [35] Sil'chenko O.K., Kuposov S.E., Vlasyuk V.V., Spiridonova O.I. *Astronomy Reports* **47**, 88 (2003)
- [36] Kassin S.A., de Jong R.S., Weiner B.J. *Astrophys. J.* **643**, 804 (2006)
- [37] Monnet G., Simien F. *Astron. Astrophys.* **56**, 173 (1977)
- [38] de Vaucouleurs G., de Vaucouleurs A. Corwin H.G., Jr., et al. "Third Reference Catalogue of Bright Galaxies. Volume I: Explanations and References". New York: Springer (1991)
- [39] Neistein E., Maoz D., Rix H.-W., Tonry J.L. *Astron. J.* **117**, 2666 (1999)
- [40] Worthey G. *Astrophys. J. Suppl. Ser.* **95**, 107 (1994)
- [41] Zamorano J., Rego M., Gallego J., et al. *Astrophys. J. Suppl. Ser.* **95**, 387 (1994)
- [42] Kalloghlian A.T., Nikoghossian E.H. *Astrophysics* **36**, 193 (1994)